OPEN ACCESS
IOP Publishing
Classical and Quantum Gravity
Class. Quantum Grav. **34** (2017) 145001 (10pp)
https://doi.org/10.1088/1361-6382/aa7119

Demonstration of the optical AC coupling technique at the advanced LIGO gravitational wave detector

Steffen Kaufer[1], Marie Kasprzack[2], Valera Frolov[3] and Benno Willke[1]

[1] Max Planck Institute for Gravitational Physics (Albert Einstein Institute), D-30167 Hannover, Germany
[2] Louisiana State University, Baton Rouge, LA 70803, United States of America
[3] LIGO Livingston Observatory, Livingston, LA 70754, United States of America

E-mail: steffen.kaufer@aei.mpg.de

Received 21 February 2017, revised 13 April 2017
Accepted for publication 4 May 2017
Published 20 June 2017

Abstract

Lasers for gravitational wave detectors need to fulfill tight requirements in amplitude stability, which can only be met by means of feedback control loops. Ultimately, power stabilization control loops are limited by the shot noise of their sensor. The power noise increases linearly with the amount of detected power, while the shot noise grows with the square root. Increasing the detected power is therefore a suitable means to reach a lower sensing noise but it is limited by the power handling capabilities of the photodiodes.

An alternative way of improving the sensitivity is the optical AC coupling technique, which exploits the high pass behavior of an optical resonator to reduce the optical power on the detector without compromising its sensitivity above the corner frequency.

In this paper we investigate the optical AC coupling technique at the aLIGO Livingston gravitational wave detector. We measured an optical AC coupling gain of 10 dB in the gravitational wave detection band, which offers the potential to improve the laser power stability by the same factor.

Keywords: optical AC coupling, power stabilization, gravitational wave detector, shot noise

(Some figures may appear in colour only in the online journal)

1. Introduction

The first detection of gravitational waves in 2015 started the age of gravitational wave astronomy [1, 2]. Current gravitational wave interferometers are large-scale Michelson interferometers enhanced with advanced interferometry techniques like signal and power recycling or arm cavities [3]. The interferometers transfer a differential phase modulation induced by a gravitational wave into a power modulation at the output port.

In the second generation gravitational wave detectors several effects induce a coupling from technical laser power noise into the readout channel of the interferometers [4–6]. The DC readout scheme [7] induces the dominant coupling for high frequencies, while radiation pressure differences in the arm cavities caused by mirror imperfections have the strongest impact at low frequencies [8].

The relative power stability reached by the currently used feedback control loops is limited by their detector shot noise. Since the relative shot noise falls with the square root of the detected optical power, detecting more power can lower this limitation. Unfortunately, commercially available photodiodes become unreliable if they have to handle too much power. To reach the required relative power noise of $2 \cdot 10^{-9}\,\mathrm{Hz}^{-1/2}$ at 10 Hz a shot noise limited photodiode array, detecting 200 mW, had to be developed [9]. While it will become increasingly difficult to reach better stabilities by detecting more optical power, alternative techniques become more attractive.

The optical AC coupling (OAC) technique can improve the sensitivity of a detector compared to its classical shot noise limitation without increasing the amount of detected power [10, 11]. The idea of OAC is to place the detector of the power stabilization feedback control loop in reflection of a narrow linewidth resonator. The optical high pass behavior of the resonator concerning noise sidebands on the reflected light is then used to change the signal to shot noise ratio on the detector.

OAC could provide a suitable way to satisfy the stability requirements of future gravitational wave detectors like the Einstein telescope [12] without developing increasingly complex photodiode arrays.

It was already demonstrated in table top power stabilization experiments, decreasing sensor noise for frequencies above 100 kHz [13]. An improvement for lower frequencies was prevented by the broad bandwidth of the resonators used in these experiments.

Here we investigated the OAC technique at the aLIGO Livingston detector. The aLIGO detectors inherently provide resonators with low linewidth, due to the 4 km armlength of the interferometer and the recycling techniques mentioned above.

We report on the first measurement of an optical AC coupling transfer function in the gravitational wave detection band, performed at the aLIGO Livingston gravitational wave detector.

Our measurement demonstrates a 10 dB increased signal to shot noise ratio for a power noise sensor using OAC compared to a classical detection scheme. It marks the first step towards an implementation of OAC at gravitational wave detectors.

We will start this article with a summary about the optical AC coupling theory before we describe how we measured the OAC transfer function at the aLIGO Livingston detector. After an overview of the parameters included in the calibration our results and the consequences for gravitational wave detectors will be discussed.

2. Optical AC coupling

The basic idea of optical AC coupling is simple: the detector of the power stabilization feedback control loop is placed in reflection of an impedance matched optical resonator with a narrow linewidth. When the laser light is resonant in the cavity the carrier light in reflection

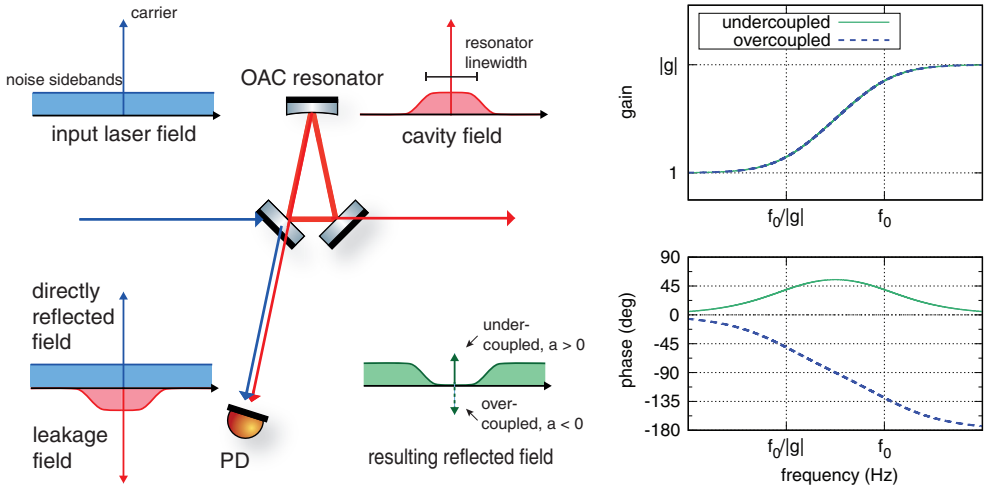

Figure 1. Left: optical AC coupling illustration in the sideband picture. The carrier light field with white noise sidebands is shining onto a locked resonator. The carrier and the sidebands within the linewidth of the resonator enter the cavity and are enhanced resonantly. The field in reflection is composed of the field directly reflected at the input mirror and the field leaking out of the cavity into the reflection port. The impedance matching then determines the phase relation between carrier component and noise sidebands in reflection of the resonator. Right: transfer function from relative power fluctuations on the incoming beam to relative power fluctuations in reflection of a cavity with corner frequency f_0.

is suppressed. This is due to destructive interference between the directly reflected field and the fraction of the circulating field that leaks into the reflection port. The amplitude noise sidebands above the resonator linewidth, however, are fully reflected and hence preserved at their original size.

The field amplitude $U_{\mathrm{in}}(f)$ of an amplitude modulated laser beam incident to a resonator can be denoted as:

$$U_{\mathrm{in}}(f) = (U_0 + U_1)(1 + \underbrace{\frac{m}{2}\mathrm{e}^{-\mathrm{i}2\pi ft}}_{M^-} + \underbrace{\frac{m}{2}\mathrm{e}^{\mathrm{i}2\pi ft}}_{M^+}) \tag{1}$$

The modulation index is given by m, while the frequency of the amplitude modulation is denoted by f. U_0 is the portion of $U_{\mathrm{in}}(f)$ which is resonant in the optical resonator. Therefore U_1 represents non resonant portion of $U_{\mathrm{in}}(f)$, which consists of higher order TEM modes as well as RF-sidebands. U_0 and U_1 are connected due to the finite total optical power P_0 and the mode matching coefficient p.

$$P_0 = U_0^2 + U_1^2 \qquad U_0^2 = (1-p)P_0 \qquad U_1^2 = pP_0 \tag{2}$$

For improved readability the lower and upper sidebands will be denoted with M^- and M^+ respectively.

The filter effect of an optical resonator with corner frequency f_0 for amplitude modulations is described by $h(f) = 1/(1 + i(f/f_0))$. The linewidth is the full width at half maximum of the resonator's transmission (see figure 1), while the corner frequency f_0 is the half width at half maximum.

The reflected field amplitude $U_{\mathrm{refl}}(f)$ for high mirror reflectivities, is deduced by adding up the directly reflected field and the leakage field of the resonator (see figure 1). The leakage field is weighted with $h(f)$, which affects the noise sidebands only.

$$U_{\mathrm{refl}}(f) = aU_0 + U_1 + [(1-(1-a)h^*(f))U_0 + U_1]M^- + [(1-(1-a)h(f))U_0 + U_1]M^+ \tag{3}$$

The impedance matching a describes the ratio between the carrier field of the incoming beam and the carrier field of the resulting reflected field [13, 14]. It depends on the cavity mirror reflectivities and the internal losses such as scattering and aperture losses due to the finite mirror size.

A negative impedance matching indicates a 180° phase difference between the carrier of the resulting field and the carrier of the incoming field. This occurs when the leakage field is larger than the directly reflected field and is referred to as the overcoupled impedance matching. A positive impedance matching means both carrier components have the same phase, which is referred to as undercoupled impedance matching.

The photodetector will sense power fluctuations instead of amplitude fluctuations. Therefore the powers $P_{\mathrm{in}}(f) = U_{\mathrm{in}}(f)\cdot U^*_{\mathrm{in}}(f)$ and $P_{\mathrm{refl}}(f) = U_{\mathrm{refl}}(f)\cdot U^*_{\mathrm{refl}}(f)$ have to be derived. For small modulations $m \ll 1$ terms of order m^2 can be neglected:

$$P_{\mathrm{in}}(f) = \underbrace{({U_0}^2 + {U_1}^2)}_{P_{\mathrm{in,DC}}} + \underbrace{2\ ({U_0}^2 + {U_1}^2)\ (M^- + M^+)}_{P_{\mathrm{in,AC}}} \tag{4}$$

With the attenuation factor K and the phase κ, both depending on a, p, f_0 and f the reflected power is:

$$P_{\mathrm{refl}}(f) = \underbrace{a^2U_0^2 + U_1^2}_{P_{\mathrm{refl,DC}}} + \underbrace{2\ K\ (M^-\mathrm{e}^{-\mathrm{i}\kappa} + M^+\mathrm{e}^{\mathrm{i}\kappa})}_{P_{\mathrm{refl,AC}}} \tag{5}$$

The transfer function of relative power fluctuations on the incoming beam to relative power fluctuations on the reflected beam (see figure 1) is given by [13]:

$$G_{\mathrm{oac}}(f) = \frac{P_{\mathrm{refl,AC}}}{P_{\mathrm{refl,DC}}} \Bigg/ \frac{P_{\mathrm{in,AC}}}{P_{\mathrm{in,DC}}} = g - (g-1)\ h(f). \tag{6}$$

$G_{\mathrm{oac}}(f)$ will be referred to as optical AC coupling transfer function. The factor g is a measure for the maximal gain in sensitivity and will therefore be referred to as optical AC coupling gain. Its value depends on the resonator's impedance matching a and its non resonant mode content p as follows:

$$g(a,p) = \frac{p + a(1-p)}{p + a^2(1-p)}. \tag{7}$$

The maximum gain is reached for frequencies above the corner frequency of the resonator, but the improvement in sensitivity can be up to 3 dB at $f = f_0/g$.

Gravitational wave detectors have their most stringent power stability requirements at low frequencies. For aLIGO these requirements are set to be a relative power noise of $2\cdot 10^{-9}$ $\mathrm{Hz}^{-1/2}$ at 10 Hz [15]. To make efficient use of the optical AC coupling technique in a gravitational wave detector a resonator with a corner frequency smaller than 10 Hz is necessary. Due to the 4 km long arm cavities and the recycling techniques used to increase the sensitivity, the aLIGO detectors inherently provide such a resonator. The interferometer which is working close to the dark fringe and is enhanced with signal recycling as well as arm cavities can be

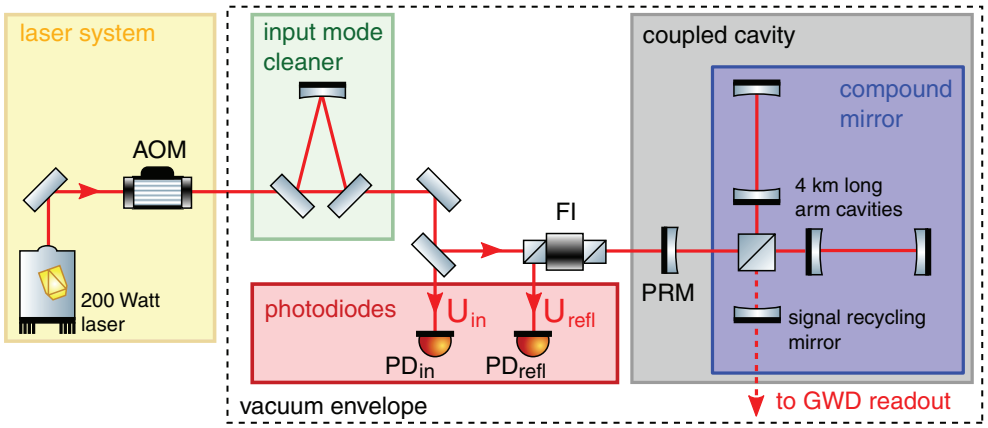

Figure 2. Simplified aLIGO setup illustrating the measurement points for the incoming and reflected beam as well the acousto-optic modulator (AOM), which was used for the amplitude modulation. The coupled cavity is formed by the power recycling mirror (PRM) and the interferometer, which can be handeled as a compound mirror. The incoming field U_{in} is picked off downstream of the input mode cleaner with $\mathrm{PD_{in}}$. The reflected field U_{refl} is measured at the Faraday isolator (FI) with $\mathrm{PD_{refl}}$

seen as a compound mirror. This compound mirror and the power recycling mirror form the so called coupled cavity with a corner frequency of approximately 0.6 Hz.

Measuring an optical AC coupling transfer function at the aLIGO detectors requires two photodetectors and an amplitude modulator. When the laser beam is resonant in the coupled cavity the amplitude modulator is used to imprint amplitude modulations. The first photodetector is used to sense the modulations incident to the coupled cavity, while the second one detects the modulation in its reflection. The optical AC coupling transfer function is measured as transfer function from power modulation on $\mathrm{PD_{in}}$ to power modulation on $\mathrm{PD_{refl}}$ (see equation (6)).

3. Experimental setup

Our experiment was performed at the aLIGO Livingston gravitational wave detector. A simplified sketch of the optical setup can be found in figure 2.

The laser beam coming from the 200 W laser system is passing through an acousto-optic modulator (AOM). The AOM is an integral part of the laser system, located outside the aLIGO vacuum system. It is used as the actuator for the power stabilization feedback control loop and can be utilized to imprint additional power modulations for our transfer function measurement.

After entering the vacuum envelope the beam is transmitted through the suspended input mode cleaner (IMC), a 16.7 m long, three mirror resonator with a Finesse of 515 [16]. After transmission through a Faraday isolator (FI) the beam enters the coupled cavity formed by the power recycling mirror (PRM) and the 4 km arm length interferometer.

The interferometer comprised of the beamsplitter and the arm cavities is stabilized to the dark fringe operation point, such that almost all light is reflected back towards the input port. Hence the interferometer can be described by a compound mirror forming the second mirror of the coupled cavity.

The first photodiode, PD_{in}, is used to measure power modulation incident to the coupled cavity. It is located in transmission of an alignment mirror, downstream of the IMC

The second photodiode, PD_{refl}, detects the light reflected from the coupled cavity, which is separated from the incoming beam by the Faraday isolator.

These two photodiodes are used to compute the OAC transfer function $G_{oac}(f)$ (see equation (6)).

Both photodiodes were already installed as a part of the standard aLIGO optical layout and hence ready to be used for our transfer function measurement without further modifications. PD_{refl} is normally used to create error signals for the common arm length degree of freedom (DOF) and the signal recycling cavity length DOF [17]. PD_{in} is usually used as a sensor of the power stabilization feedback control loop. The feedback control loop had to be disabled for our transfer function measurement, otherwise the imprinted modulation would have been suppressed.

4. Measurement and calibration

This section will give a brief summary of the measurement and calibration procedure.

Both photodiodes, PD_{in} and PD_{refl}, produce different voltages for a specific power modulation imprinted by the AOM. For the purpose of this paper a relative calibration between both photodiodes was necessary.

Therefore the central beamsplitter of the Michelson interferometer was intentionally misaligned. In this situation the light can not become resonant in the interferometer and the power recycling mirror reflects all incoming light. The AOM was now used to imprint amplitude modulations required to measure a transfer function $H_{unlockled}(f)$ between the two photodiodes. This transfer function gives a precise calibration factor $\alpha(f) = 1/H_{unlockled}(f)$ regarding optical and electronic gain differences between them.

With the whole interferometer locked the transfer function $H_{lockled}(f)$ was measured to estimate the OAC transfer function. While the DC power on PD_{in} is unchanged in this situation, the DC power on PD_{refl} changes significantly due to the carrier light suppression g_{red}. The carrier light suppression depends on the mode matching coefficient p and the impedance matching a and can be measured directly with PD_{refl} :

$$g_{red} = \frac{P_{refl,DC,locked}}{P_{refl,DC,unlocked}} = a^2(1-p) + p \tag{8}$$

Following equation (6) the OAC transfer function can be calculated from $H_{lockled}(f)$ via:

$$G_{oac}(f) = \frac{P_{refl,AC}}{P_{in,AC}} \cdot \frac{P_{refl,DC}}{P_{in,DC}} = \alpha(f) \cdot H_{lockled}(f) \ / \ g_{red} \tag{9}$$

To measure the optical AC coupling transfer function we used two different techniques. For frequencies above 5 Hz we used a broadband modulation with modulation coefficients of the order $m = 5 \cdot 10^{-3}$. For frequencies in between 0.1 Hz and 100 Hz we chose to use single frequency modulations instead of broadband modulations. This choice was motivated by higher noise levels on the light reflected by the coupled cavity and the existence of several mechanical resonance frequencies of the mirror suspensions in this frequency range. These resonances could have been excited by a broadband modulations via radiation pressure effects. We chose the modulation frequencies such that mechanical resonances were avoided and used modulation coefficients up to $m = 0.02$ to overcome the excess noise.

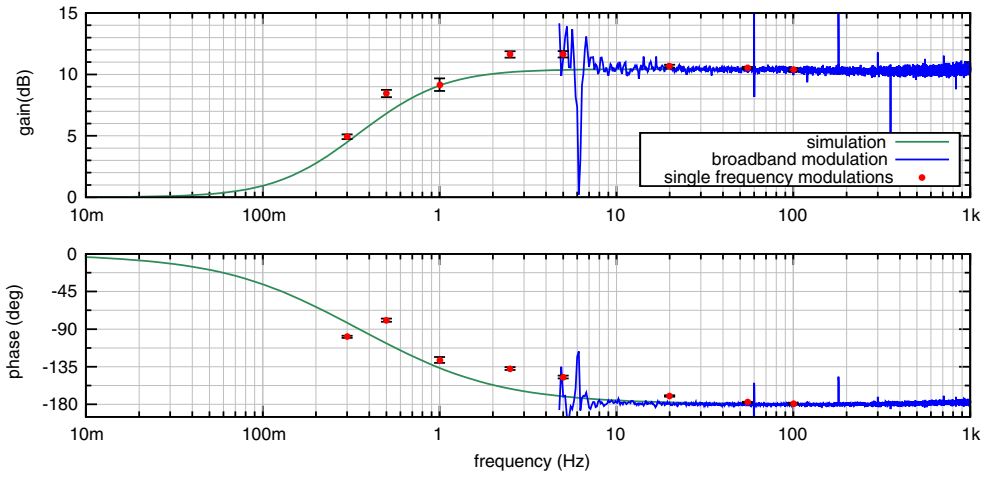

Figure 3. Measurement of the optical AC coupling transfer function, blue: broadband modulations for frequencies above 5 Hz, red: single frequency modulations with error bar in black, green: theoretical optical AC coupling transfer function for derived optical AC coupling gain and simulated corner frequency.

Whenever a transfer function H_{xy} between two signals $x(f)$ and $y(f)$ is measured, the estimate $\hat{H}_{xy}$ of the transfer function comes with a statistical error. Assuming an unbiased measurement the normalized rms error ϵ for the gain estimate $|\hat{H}_{xy}|$ can be determined via the coherence γ^2_{xy} between both signals and the number of averages n_D [18]:

$$\epsilon[|\hat{H}_{xy}|] = \frac{\text{s.d.}[|\hat{H}_{xy}|]}{|H_{xy}|} = \frac{(1-\gamma^2_{xy})^{1/2}}{|\gamma_{xy}|\sqrt{2\,n_D}} \tag{10}$$

The error in the phase estimate $\hat{\Phi}_{xy}$ in radians can be found to match the standard deviation (s.d.) when ϵ is small :

$$\text{s.d.}[\hat{\Phi}_{xy}] \approx \epsilon[|H_{xy}|] \tag{11}$$

Consequently the coherence was measured in parallel to the transfer function measurement. A very strong coherence could be measured for the broadband modulations above 20 Hz. Therefore a statistical error of $\epsilon \leqslant 0.125$ dB and $\text{s.d.}[\hat{\Phi}_{xy}] \leqslant 0.8°$ could be derived. The modulation strength and the number of averages was then adjusted to yield at least $\epsilon < 1$ dB for every single frequency modulation measurement. The error bars for the measurements in figure 3 are derived using the measured coherence and number of averages and represent the individual statistical errors for each modulation frequency.

5. Results and simulation

In figure 3 we present a Bode diagram of the broadband optical AC coupling transfer function measurement (blue) as well as the single frequency modulation measurements (red). There are two major findings from this measurement: the optical AC coupling gain is $g = 10.43$ dB and the coupled cavity is in an overcoupled state. The overcoupled state manifests itself in the phase behavior of the transfer function measurement. The phase flip of 180° between frequencies below and above the corner frequency is characteristic for overcoupled cavities.

Table 1. Power reduction g_{red}, impedance matching a, non resonant mode content p and optical AC coupling gain g, derived from the measurements and predicted via simulations.

	g_{red}	a	p	g (dB)
Preestimation	0.0147	−0.068	0.01	11.16
Measured	0.01209	−0.050	0.0096	10.43

The carrier field in reflection is dominated by the carrier light leaking out of the resonator, which has a phase of 180° compared to the directly reflected noise sidebands outside the cavity linewidth (see figure 1).

To compare our results with the OAC theory we had to estimate several parameters of the coupled cavity. Hence an Optickle simulation [19] of the complete optical setup was performed. Based on our knowledge of the interferometer we estimated a corner frequency $f_0 = 0.64$ Hz, a mode matching coefficient p and an impedance matching a (see table 1). These estimates directly inferred a predicted carrier reduction g_{red} and an OAC gain g.

In a second step we calculated a set of parameters p, and a from our measurements. Therefore we relied on the fact that independent measurements of the carrier reduction g_{red} and the optical AC coupling gain g allow to estimate the impedance matching a as well as the mode matching coefficient p.

We measured the carrier reduction g_{red} and OAC gain g as described in the section 3. With the equations (7) and (8) the parameters a and p were estimated. Our predicted values for impedance matching, non resonant mode content, power reduction and OAC gain are compared to the values resulting from the measurements in table 1. The preestimated and measured parameters are in close agreement with each other. We then used our measured optical AC coupling gain g and the simulated corner frequency to calculate the theoretical curve shown in green in figure 3.

The measured transfer function agrees with the theoretical curve for high frequencies regarding its flat behavior. The measured data for frequencies below 5 Hz, however, deviates from the predicted OAC transfer function stronger than the derived statistical errors for an unbiased measurement can explain.

6. Discussion

The single frequency modulations yield very consistent results with the broadband measurements, therefore a qualitative difference of both measuring methods could mostly be ruled out. The deviation between our data and the theoretical transfer function at low frequencies could not be fully explained by the statistical errors of the measurements. However, in a gravitational wave detector with its numerous feedback control loops, other couplings could be the cause of this deviation.

Such a coupling could, for example, be caused by the differential arm length control loop. The interferometer is using a DC readout scheme, which means that the power level at the output port is used as an error signal to control the differential arm length degree of freedom. Therefore an injected power modulation which is transferred through the complete interferometer would be interpreted as a differential arm length change. The control loop would try to counteract this power change by acting on the testmasses, this could produce additional modulation in reflection of the interferometer. Such couplings are not included in our simulations but have the potential to bias the measurement. Further investigations about additional

couplings of power modulations on the incoming beam to power modulations in reflection of the coupled cavity should be performed.

Our measurements show the potential of the optical AC coupling technique for future improvements in power stabilization feedback control loops. Including the OAC technique at aLIGO could improve the shot noise limited power stability by 10 dB compared to the classical detection scheme which is currently used.

The implementation of OAC into a working power stabilization concept comes with relatively small additional effort. The only requirement for implementation is a low noise photodiode in the reflection port of the power recycling cavity. Since the aLIGO power stabilization is remote controlled, an OAC loop could be set up in parallel to the traditional stabilization and then be used as a test environment for a detailed noise analysis of this technique. Even though relative intensity noise is not a limiting noise source in the current state of the aLIGO detectors, the possibility to switch to an OAC based stabilization would help on further investigating OAC under realistic environmental conditions, especially regarding additional sensor noise attributed to OAC. As a first step this detector could be set up outside of the vacuum system, nevertheless using an in vacuum detector could be beneficial regarding pointing and scattering effects.

Third generation gravitational wave observatories like ET [12] or the newly proposed speed meter topology [20] rely on the use of power recycling resonators. This means OAC will stay a viable option for future gravitational wave detectors, since narrow linewidth resonators will be available.

7. Conclusion

We demonstrated the first measurement of an optical AC coupling transfer function at a gravitational wave detector. The optical AC coupling gain at the aLIGO Livingston detector was found to be $g = 10.43$ dB, which is in close agreement with simulations. To reach an equivalent enhancement in signal to shot noise ratio without OAC the detected power would need to be increased by a factor of 10. The effort to produce a complex photodiode array, capable of detecting such an increased power level, would be very high.

The shape of the transfer function follows theory closely, having small deviations at low frequencies. These deviations might be caused by couplings not included into our simulations, like the influence of other feedback control loops.

An implementation of optical AC coupling into a power stabilization feedback control loop at the aLIGO detectors comes with small experimental effort. It would provide great additional information about potential noise sources of OAC in a realistic test bed. The presented measurements demonstrated the large potential of OAC for third generation GWDs and should encourage further investigations.

Acknowledgments

The authors want to acknowledge useful discussion with Anamaria Effler and Brian O'Reilly. Thanks to Keiko Kokeyama for the aLIGO Optickle script, which was used for our simulations. LIGO was constructed by the California Institute of Technology and Massachusetts Institute of Technology with funding from the National Science Foundation. It operates under Cooperative Agreement No. PHY-0757058. Advanced LIGO was built under Grant No. PHY-0823459. MK wants to acknowledge NSF Grant No. PHY-1505779 and Grant

No. PHY-1205882. The corresponding author was supported by the Max Planck Society, Germany, and the LSC Fellows program. The LIGO Document Number of this document is LIGO-P1700010.

References

[1] Abbott B P *et al* (LIGO Scientific Collaboration and Virgo Collaboration) Observation of gravitational waves from a binary black hole merger *Phys. Rev. Lett.* **116** 061102
[2] Einstein A 1918 *Ueber Gravitationswellen* (*Preussische Akademie der Wissenschaft*) (Berlin: Verlag der Königlichen Akademie de Wissenschaften) p 154
[3] Strain K A and Meers B J 1991 Experimental demonstration of dual recycling for interferometric gravitational-wave detectors *Phys. Rev. Lett.* **66** 1391–4
[4] Harry G M and The LIGO Scientific Collaboration 2010 Advanced LIGO: the next generation of gravitational wave detectors *Class. Quantum Grav.* **27** 084006
[5] Acernese F and The Virgo Collaboration 2015 Advanced Virgo: a second-generation interferometric gravitational wave detector *Class. Quantum Grav.* **32** 024001
[6] Willke B *et al* 2006 The GEO-HF project *Class. Quantum Grav.* **23** 207–14
[7] Fricke T *et al* 2012 DC readout experiment in enhanced ligo *Class. Quantum Grav.* **29** 065005
[8] Willke B, King P, Savage R and Fritschel P 2011 Pre-stabilized laser design requirements LIGO DCC https://dcc.ligo.org/LIGO-T050036-v2/public
[9] Kwee P, Willke B and Danzmann K 2009 Shot-noise-limited laser power stabilization with a high-power photodiode array *Opt. Lett.* **34** 2912–14
[10] Kwee P, Willke B and Danzmann K 2009 Laser power stabilization using optical ac coupling and its quantum and technical limits *Appl. Opt.* **48** 5423–31
[11] Kwee P, Willke B and Danzmann K 2008 Optical ac coupling to overcome limitations in the detection of optical power fluctuations *Opt. Lett.* **33** 1509–11
[12] Einstein gravitational wave Telescope Conceptual Design Study, The ET science team 2011 https://tds.ego-gw.it/ql/?c=7954
[13] Kwee P 2010 Laser characterization and stabilization for precision interferometry *PhD Thesis* Leibniz Universitaet Hannover
[14] Siegman A E 1986 *Lasers* (Mill Valley, CA: University Science Books)
[15] Shoemaker D 2011 Advanced LIGO Reference Design LIGO DCC https://dcc.ligo.org/LIGO-M060056/public
[16] Mueller C L *et al* 2016 The advanced ligo input optics *Rev. Sci. Instrum.* **87** 014502
[17] Peter Fritschel J R 2014 List of ISC photodetectors in advanced LIGO DCC T1000264-v7 https://dcc.ligo.org/LIGO-T1000264/public
[18] Bendat J S and Piersol A G 2000 *Random Data: Analysis and Measurement Procedures* (New York: Wiley)
[19] Evans M 2016 Optickle *Technical Report* LIGO Document T070260-v1 2016 https://dcc.ligo.org/T070260/public
[20] Hild S 2012 Beyond the second generation of laser-interferometric gravitational wave observatories *Class. Quantum Grav.* **29** 124006